Title

Prediction of spatially variable unsaturated hydraulic conductivity using scaled particle-size distribution functions

Journal

Water Resources Research, 49(7)

ISSN

0043-1397

Authors

Nasta, Paolo
Romano, Nunzio
Assouline, Shmuel
et al.

Publication Date

2013-07-01

DOI

10.1002/wrcr.20255

Peer reviewed

WATER RESOURCES RESEARCH, VOL. 49, 4219–4229, doi:10.1002/wrcr.20255, 2013

Prediction of spatially variable unsaturated hydraulic conductivity using scaled particle-size distribution functions

Paolo Nasta,[1,4] Nunzio Romano,[2] Shmuel Assouline,[3] Jasper A. Vrugt,[4] and Jan W. Hopmans[5]

Received 12 September 2012; revised 10 April 2013; accepted 12 April 2013; published 26 July 2013.

[1] Simultaneous scaling of soil water retention and hydraulic conductivity functions provides an effective means to characterize the heterogeneity and spatial variability of soil hydraulic properties in a given study area. The statistical significance of this approach largely depends on the number of soil samples collected. Unfortunately, direct measurement of the soil hydraulic functions is tedious, expensive and time consuming. Here we present a simple and cost-effective hybrid scaling approach that combines the use of ancillary information (e.g., particle-size distribution and soil bulk density) with direct measurements of saturated soil water content and saturated hydraulic conductivity. Our results demonstrate that the presented approach requires far fewer laboratory measurements than conventional scaling methods to adequately capture the spatial variability of soil hydraulic properties.

Citation: Nasta, P., N. Romano, S. Assouline, J. A. Vrugt, and J. W. Hopmans (2013), Prediction of spatially variable unsaturated hydraulic conductivity using scaled particle-size distribution functions, *Water Resour. Res.*, *49*, 4219–4229, doi:10.1002/wrcr.20255.

1. Introduction

[2] The predictive ability and utility of large-scale distributed hydrologic models heavily relies on a detailed description of the spatial variability of the soil hydraulic properties, namely the water retention function (WRF) and the unsaturated hydraulic conductivity function (HCF). The WRF relates the volumetric water content θ (L^3 L^{-3}) to the corresponding soil water matric head h (L). The HCF relates the unsaturated hydraulic conductivity K (L T^{-1}) to the soil matric head or water content. The spatial distribution of WRF and HCF can be characterized with effective soil hydraulic parameters [*Zhu and Mohanty*, 2002; *Zhu and Mohanty*, 2003; *Vrugt et al*., 2004; *Mohanty and Zhu*, 2007]. Although this approach provides a reasonable description of the lumped behavior of the soil system, it does not accurately characterize the inherent spatially distributed soil water fluxes.

[3] In the past decades, the scaling approach has been developed as an effective method to describe the spatial variability of the soil hydraulic properties in a given study area [*Warrick and Nielsen*, 1980; *Tillotson and Nielsen*, 1984; *Clausnitzer et al*., 1992]. This approach was introduced in soil physics by the seminal paper of *Miller and Miller* [1956] and is based on the assumption that geometrically similar porous media differ only by a characteristic length of their respective pore-size distributions, which in turn provide a good proxy for the soil hydraulic properties. Spatial variability is defined through the statistical distribution of scaling factors that relate the soil hydraulic functions sampled in different locations to the corresponding average hydraulic properties of a reference porous medium (representative for the study area). This geometric scaling approach has been successfully applied for Kosugi's soil hydraulic functions [*Kosugi*, 1996], assuming that scaling factors are lognormally distributed in the sampled soil domain. This includes individual scaling of soil WRFs only [*Kosugi and Hopmans*, 1998; *Hayashi et al*., 2009] or simultaneous scaling of soil water retention and unsaturated HCFs [*Hendrayanto et al*., 2000; *Tuli et al*., 2001].

[4] Notwithstanding this progress made, the inherent spatial variability of soils necessitates a very large number of samples to accurately characterize the hydraulic properties of the considered spatial domain [*Hopmans et al*., 2002a; *Minasny and McBratney*, 2007; *Vereecken et al*., 2007]. Unfortunately, direct measurement of the soil hydraulic properties (hereafter referred to as primary data or PD) is time consuming and tedious [*Hopmans et al*., 2002b]. Alternatively, pedotransfer functions (PTFs) can be used to indirectly estimate the soil hydraulic functions from soil physical and chemical data (hereafter defined as secondary data or SD) that are more readily available because of their ease in collection and simplicity in measurement [*Haverkamp et al*., 2002]. Most PTFs estimate the soil hydraulic functions through mathematical and statistical relations by using oven-dry bulk density, organic carbon content, and soil texture [*Pachepsky and Rawls*, 2004]. We emphasize that PTFs necessitate empirical

[1]Department of Earth and Atmospheric Sciences, University of Nebraska, Lincoln, Nebraska, USA.
[2]Department of Agriculture, Division of Agricultural, Forest and Biosystems Engineering, University of Napoli Federico II, Portici, Naples, Italy.
[3]Department of Environmental Physics and Irrigation, A.R.O, Volcani Center, Bet Dagan, Israel.
[4]Department of Civil and Environmental Engineering, University of California, Irvine, California, USA.
[5]Department of Land, Air and Water Resources, University of California, Davis, California, USA.

Corresponding author: P. Nasta, Department of Earth and Atmospheric Sciences, University of Nebraska, Lincoln, NE 68588, USA. (paolo.nasta@unina.it)

0043-1397/13/10.1002/wrcr.20255

calibration procedures, and their validity is restricted only for the tested database [*Chirico et al*., 2007]. The majority of PTFs presented in the literature use simple nonlinear regression equations to relate the hydraulic properties to basic soil texture and structure data [*Tietje and Tapkenhinrichs*, 1993; *Weynants et al*., 2009; *Vereecken et al*., 2011]. Such equations are easy to implement and are often favored over more complex fitting methods, such as artificial neural networks [*Schaap and Bouten*, 1996; *Schaap et al*., 1998].

[5] Although PTFs may provide good estimates of the soil hydraulic properties [*Romano*, 2004], they depend on empirical relationships that do not offer physical understanding in the interpretation of their flaws [*Haverkamp et al*., 2002]. Alternatively, physical-empirical PTFs rely on pore-scale physical relationships that are adjusted through empirical calibrations [*Chan and Govindaraju*, 2004; *Hwang and Choi*, 2006; *Nimmo et al*., 2007]. Specifically, *Arya and Paris* [1981] proposed a method (hereinafter defined as AP method) to estimate the soil pore-size distribution by using the soil particle-size distribution (PSD) and oven-dry bulk density. The AP method postulates the fundamental assumption of shape similarity between WRF and PSD. The soil is described as an ideal porous medium with modeled pore spaces created by a cubic packing of uniform spheres. The actual soil matrix geometry is adjusted by an empirical parameter α that corrects for the differences in shape and spatial arrangement of solid particles between hypothetical and actual porous medium [*Arya et al*., 1999a, 2008]. Although *Arya and Paris* [1981] assumed a constant α value of 1.38 for coarse porous media, others proposed to vary α as a function of matric head [*Basile and D'Urso*, 1997], particle size [*Buczko and Gerke*, 2005], or water content [*Vaz et al*., 2005] of the soil. The AP method has subsequently been upgraded by adding the prediction of unsaturated hydraulic conductivity as well [*Arya et al*., 1999b; *Chaudhari and Batta*, 2003; *Hwang and Hong*, 2006; *Blank et al*., 2007; *Arya and Heitman*, 2010]. More recently, *Nasta et al*. [2009] proposed a geometric scaling method of the WRFs estimated with the AP method. This work relaxes experimental effort as the calibration of the parameter α requires only a limited number of direct measurements of the WRF of soil samples within the sampled spatial domain.

[6] In this paper we present a hybrid simultaneous scaling approach that complements SD (PSD and oven-dry bulk density) with easily obtainable PD (saturated water content and saturated hydraulic conductivity) to assess the spatial variability of both WRF and HCF. The main purpose of this work is to offer a methodological approach to significantly reduce experimental effort.

[7] The remainder of this paper is organized as follows. In section 2.1, the conventional simultaneous scaling method is described using laboratory measurements of the soil hydraulic properties (PD) to obtain the reference soil WRF (REF-WRF_{PD}) and HCF (REF-HCF_{PD}), respectively, and the corresponding scaling factors δ_{PD} [*Tuli et al*., 2001]. Section 2.2 then proceeds with the introduction of our hybrid simultaneous scaling method that uses measurements of the PSD and bulk density (SD) jointly with data of the saturated water content (θ_s) and saturated hydraulic conductivity (K_s) (PD) to estimate the reference soil WRF (REF-WRF_{SD}) and HCF (REF-HCF_{SD}), respectively, and the corresponding scaling factors δ_{SD}. The experimental data are subsequently described in section 3. In section 4, the results of our new hybrid scaling approach are compared against those of the conventional scaling method. Finally, section 5 concludes with a summary of the analysis presented herein.

2. Theory

2.1. Simultaneous Scaling Using PD

[8] Assuming soil to be represented by a randomly distributed bundle of intersecting cylindrical capillary tubes (series-parallel statistical model) with a probability density function (pdf) of soil pore radii pdf(r) (L^{-1}), the volumetric water content of the water-filled pores of radii $r \rightarrow r+\mathrm{d}r$ is computed from $\mathrm{d}\theta(r) = \mathrm{pdf}(r)\mathrm{d}r$ (L^{-1} L) [*Brutsaert*, 2000]. *Kosugi* [1996] proposed to describe the pdf(r) function using a log-normal probability law with mean ln r_m (ln indicates the natural logarithm) and standard deviation (STD) σ:

$$\mathrm{pdf}(\ln r) = \frac{\theta_s - \theta_r}{r\sigma\sqrt{2\pi}} \exp\left[-\frac{(\ln r - \ln r_m)^2}{2\sigma^2}\right], \tag{1}$$

where θ_s (L^3 L^{-3}) and θ_r (L^3 L^{-3}) represent the saturated and residual soil water content, respectively. The soil water matric head h (L) is assumed to be proportional to the inverse of the equivalent pore radius r (L) through the Young-Laplace capillary equation (i.e., $r \approx 0.149/h$ if r and h are expressed in units of centimeters). The soil WRF $S_e(\ln h)$ is described as follows:

$$S_e(\ln h) = \frac{\theta - \theta_r}{\theta_s - \theta_r} = \frac{1}{2}\mathrm{erfc}\left[\frac{(\ln h - \ln h_m)}{\sigma\sqrt{2}}\right], \tag{2}$$

where erfc represents the complementary error function, ln h_m and σ denote the mean and STD of ln h, respectively, and S_e represents the degree of saturation that varies from 0 (when $\theta = \theta_r$) to 1 (when $\theta = \theta_s$). The h_m value is the median matric head corresponding to $S_e = 0.5$ [*Kosugi*, 1996; *Kosugi et al*., 2002].

[9] According to *Mualem* [1976], the relative hydraulic conductivity $K_r(S_e)$ is described as

$$K_r(S_e) = \frac{K(S_e)}{K_s} = T(S_e)G(S_e)\left(\frac{\int_0^{S_e}\frac{1}{h}\mathrm{d}S_e}{\int_0^1\frac{1}{h}\mathrm{d}S_e}\right)^2 = S_e^l\left(\frac{\int_0^{S_e}\frac{1}{h}\mathrm{d}S_e}{\int_0^1\frac{1}{h}\mathrm{d}S_e}\right)^2, \tag{3}$$

where K_s (L T^{-1}) denotes the saturated hydraulic conductivity, $T(S_e)$ is a tortuosity factor that corrects for the effective path length of the water-conducting noncylindrical tubes, and $G(S_e)$ accounts for the connectivity among the water-conducting pores [*Mualem*, 1976; *Touma*, 2009; *Lebeau and Konrad*, 2010]. Note that the relative hydraulic conductivity K_r varies between 0 (when $\theta = \theta_r$ or $S_e = 0$) and 1 (when $\theta = \theta_s$ or $S_e = 1$).

[10] The power of 2 in equation (3) originates from the assumption that the pore configuration can be replaced by a pair of capillary elements whose lengths are proportional to

their respective radii. *Mualem* [1976] simplified the relation in equation (3) by combining $T(S_e)$ and $G(S_e)$ into a single factor S_e^l, where the exponent l enables the tortuosity connectivity to change as a function of soil water content. The value of the power l depends on the specific soil-fluid properties and varies considerably among soils [*Peters et al*., 2011]. Based on a data set of 45 soils, *Mualem* [1976] proposed an optimal value of $l = 0.5$. However, *Leij et al*. [1997] obtained a mean value of $l = -0.72$ using another data set of 401 soils.

[11] Alternatively, *Assouline* [2001, 2005] proposed a different analytical relationship for the unsaturated HCF that incorporates the tortuosity and connectivity factors into a single power value η:

$$K_r(S_e) = \left(\frac{\int_0^{S_e} \frac{1}{h} \mathrm{d}S_e}{\int_0^1 \frac{1}{h} \mathrm{d}S_e} \right)^{\eta}. \tag{4}$$

[12] If we now insert Kosugi's water retention relation (i.e., equation (2)) into equation (4), we obtain the following expression for the relative HCF:

$$K_r(S_e) = \left\{ \frac{1}{2} \mathrm{erfc} \left[\mathrm{erfc}^{-1}(2S_e) + \frac{\sigma}{\sqrt{2}} \right] \right\}^{\eta}, \tag{5}$$

with parameter η hereafter referred to as the conductivity parameter.

[13] The scaling approach provides a convenient way to coalesce a group of j soil hydraulic properties onto a single reference hydraulic function [*Kosugi and Hopmans*, 1998; *Tuli et al*., 2001]. The reference soil WRF (REF-WRF) $\hat{S}_e(\ln h)$ and the reference relative HCF (REF-HCF) $\hat{K}_r(\hat{S}_e)$ are described by the following two parametric relations:

$$\hat{S}_e(\ln h) = \frac{1}{2} \mathrm{erfc} \left[\frac{\left(\ln h - \ln \hat{h}_m \right)}{\hat{\sigma}\sqrt{2}} \right] \tag{6}$$

and

$$\hat{K}_r(\hat{S}_e) = \left\{ \frac{1}{2} \mathrm{erfc} \left[\mathrm{erfc}^{-1}(2\hat{S}_e) + \frac{\hat{\sigma}}{\sqrt{2}} \right] \right\}^{\hat{\eta}}, \tag{7}$$

where $\ln \hat{h}_m$, $\hat{\sigma}$, and $\hat{\eta}$ are the arithmetic mean values of all $\ln h_{m,j}$, σ_j and η_j values, respectively.

[14] The geometric similarity of *Miller and Miller* [1956] dictates the median pore radius, $r_{m,j}$, as the characteristic length of the pore-size distribution of each soil sample j. The scaling approach identifies a representative pore-size distribution for the entire soil domain with corresponding mean value of $\ln r_{m,j}$ ($\ln \hat{r}_m$). Provided that $r_{m,j}$ and $h_{m,j}$ (as well as $\ln \hat{r}_m$ and $\ln \hat{h}_m$) are linked by the capillary law, the scaling factors δ_j are defined as follows [*Miller and Miller*, 1956; *Kosugi and Hopmans*, 1998]:

$$\delta_j = \frac{r_{m,j}}{\hat{r}_m} = \frac{\hat{h}_m}{h_{m,j}}. \tag{8}$$

[15] The scaling factors quantify the relative deviation (RD) of the $r_{m,j}$ values pertaining to different locations with respect to the $\hat{r}_m$ value referred to the study area. The resulting distribution of the scaling factors will be assumed lognormal with the constraint that the mean value (μ) of the log-transformed scaling factors is null, $\mu(\ln \delta_j) = 0$ [*Kosugi and Hopmans*., 1998]. Therefore, the geometric scaling describes the spatial variability of soil hydraulic properties through the reference hydraulic functions and the statistical distribution of scaling factors. A key advantage of this method is that one can directly draw scaling factors from the lognormal pdf to rapidly characterize the spatial variability of the soil hydraulic functions in large spatial domains [*Nasta et al*., 2013].

[16] The scaled soil water retention curves can now be expressed as

$$S_e[\ln(\delta_j h)] = \frac{1}{2} \mathrm{erfc} \left[\frac{\ln(\delta_j h) - \ln \hat{h}_m}{\hat{\sigma}\sqrt{2}} \right], \tag{9a}$$

and the scaled unsaturated HCFs [*Miller and Miller*, 1956; *Tuli et al*., 2001] as

$$\delta_j^{-2} K_r(S_e) = \left\{ \frac{1}{2} \mathrm{erfc} \left[\mathrm{erfc}^{-1}(2S_e) + \frac{\hat{\sigma}}{\sqrt{2}} \right] \right\}^{\hat{\eta}}. \tag{9b}$$

[17] The parameters $h_{m,j}$, σ_j, $\theta_{r,j}$, and η_j (hereafter indicated with the subscript PD) have to be estimated directly from the PD (water retention and hydraulic conductivity data points). While parameters $\theta_{s,j}$ and $K_{s,j}$ are easily measured, SD help in alleviating the demanding task of measuring the unsaturated hydraulic properties. The next section will introduce the main elements of a hybrid scaling approach that combines primary and SD to describe the spatial variability of the WRF and HCF.

2.2. Simultaneous Scaling Using SD

[18] We assume that the PSD function is described by Buchan's equation (*Buchan*, [1989], *Bah et al*. [2009], Table 2):

$$W(\ln D) = \frac{1}{2} \mathrm{erfc} \left[\frac{(\ln D_m - \ln D)}{\sigma_{\mathrm{PSD}}\sqrt{2}} \right], \tag{10}$$

where W ($M\,M^{-1}$) defines the solid mass fraction associated with particles of diameter size D (L), and $\ln D_m$ and σ_{PSD} are the mean and STD of the log-transformed soil particle diameters, respectively. Note that equation (10) has an analytical form similar to Kosugi's WRF, as defined by equation (2). The number of solid particles n_i (M^{-1}) for each soil particle diameter class i is calculated from

$$n_i = \frac{6}{\pi} \frac{W_i}{D_i^3 \rho_s}, \tag{11}$$

where ρ_s ($M\,L^{-3}$) represents the soil particle density, which hereafter is assumed to be equal to 2.65 g cm^{-3}. The pore radius r_i associated with the particle diameter D_i is calculated as follows [*Arya and Paris*, 1981]:

$$r_i = \frac{D_i}{2} \sqrt{\frac{2en_i^{(1-\alpha_i)}}{3}}, \tag{12a}$$

Table 1. Statistical Properties of Sand, Silt, and Clay Contents, Oven-Dry Bulk Density (ρ_b), and Soil Porosity (ε), and Optimized Parameters of Buchan's Relation ($\ln D_m$ and σ_{PSD}) for the 84 Soil Samples Collected in the Study Site

	Sand (%)	Silt (%)	Clay (%)	$\ln D_m$ (cm)	σ_{PSD}	ρ_b (g cm^{-3})	ε (cm^3 cm^{-3})
μ[a]	44.36	44.48	11.16	−5.64	2.36	1.14	0.54
STD	2.21	1.60	2.22	0.14	0.15	0.07	0.03
CV (%)	4.98	3.61	19.90	2.47	6.49	5.79	4.83
min	40.07	40.57	6.69	−5.94	2.04	0.96	0.49
max	49.18	47.34	15.66	−5.34	2.66	1.28	0.62

[a] μ, mean; STD, standard deviation; CV; coefficient of variation; min, minimum value; max, maximum value.

where α is an empirical parameter and e (L^3 L^{-3}) denotes the void ratio defined as

$$e = \frac{\rho_s - \rho_b}{\rho_b}, \tag{12b}$$

where ρ_b (M L^{-3}) denotes the oven-dry bulk density. It is important to point out that α maps the hypothetical simple geometry of soil particles into the actual geometry so that the particle diameter D can be converted to an equivalent pore radius r.

[19] The AP method is based on the assumption of shape similarity between PSD and WRF; hence, the W_i classes associated to the diameter class D_i are supposed equivalent to the $S_{e,i}$ classes correspondent to the pore radius class r_i. The estimated retention data pairs $S_{e,i}$-h_i (with h_i values calculated from r_i in equation (12a) using the capillary law) then serve as input for the scaling of the SD. To this end, parameters $h_{m,\mathrm{SD},j}$ and $\sigma_{\mathrm{SD},j}$ of equation (2) will be optimized for each soil sample j, and their mean values $\ln \hat{h}_{m,\mathrm{SD}}$ and $\hat{\sigma}_{\mathrm{SD}}$ will be inserted in equation (6) to obtain the reference WRF, REF-WRF$_{\mathrm{SD}}$. The HCFs for each soil sample j are derived from equation (5), while the reference HCF REF-HCF$_{\mathrm{SD}}$ and the scaling factors $\delta_{\mathrm{SD},j}$ are calculated using equations (7) and (8), respectively. Note that the parameters η and α are unknown a priori for the scaling of the SD and an empirical calibration procedure is required. This step will be described in section 4.2.1.

3. Materials and Methods

[20] The experimental area is located to the east of the city of Naples, Italy [*Romano*, 1993; *Ciollaro and Romano*, 1995]. The volcanic soil (Andosol) originated from eruptions of the Vesuvius volcano. Soil physical and hydraulic characteristics were determined from 84 undisturbed soil cores (12 cm length, 8.6 cm diameter) that were collected from the soil surface (about 10–25 cm soil depth) along a 126 m long transect with equal intervals of 1.50 m. Before conducting the soil hydraulic measurements in the laboratory, the top 2.5 cm slice of each soil core was removed for soil texture and pressure plate extraction measurements. Disturbed soil samples were repacked and placed in a pressure plate extractor to determine equilibrium soil water retention points at −3000, −6000, and −12,000 cm. The remaining portion of the disturbed samples was analyzed for determining the soil PSD [*Gee and Or*, 2002]. The sieve analysis method was used to determine the sand content with five diameter classes for $0.005\ \mathrm{cm} < D_i < 0.2\ \mathrm{cm}$, whereas the hydrometer method was used to determine the distribution of the silt and clay fractions with six diameter classes for $D_i < 0.005$ cm. Buchan's parametric relation of equation (10) was fitted to each of the 84 experimental $D_{i,j}$ (cm)-$W_{i,j}$ (g g^{-1}) data pairs using the MATLAB Optimization Toolbox (The MathWorks, Inc.) [*Coleman and Li*, 1996]. This procedure results in optimized values for $\ln D_{m,j}$ and $\sigma_{\mathrm{PSD},j}$. Table 1 summarizes the mean (μ), STD, coefficient of variation (CV), minimum (min) and maximum (max) values of the soil texture parameters, oven-dry bulk density, ρ_b (g cm^{-3}), and soil porosity, ε (cm^3 cm^{-3}). Note that these soil properties exhibit a rather low variability (see CV values in Table 1). Figure 1 presents the measured PSD functions with the average sand, silt, and clay contents of 44.4%, 44.5%, and 11.1%, respectively, and corresponding STDs of 2.2 (sand), 1.6 (silt), and 2.2 (clay).

[22] The undisturbed soil core was slowly wetted from the bottom, until reaching its complete saturation. The saturated water content θ_s (cm^3 cm^{-3}) was measured by the gravimetric method [*Topp and Ferré*, 2002], whereas the saturated hydraulic conductivity K_s (cm h^{-1}) was determined by the falling-head method [*Reynolds and Elrick*, 2002]. For each soil core, the evaporation method enabled the simultaneous determination of the soil water retention $\theta(h)$ and hydraulic conductivity $K(h)$ data points [*Wendroth et al.*, 1993; *Peters and Durner*, 2008]. During the evaporation experiments, matric head values at the soil depths of 3.0 cm and 6.0 cm were measured at irregular time intervals using horizontally inserted microtensiometers (measuring matric heads in the range of $-600\ \mathrm{cm} < h < 0$ cm) [*Ciollaro and Romano*, 1995; *Romano and Santini*, 1999].

Table 2. Mean (μ), Standard Deviation (STD), Coefficient of Variation (CV), Maximum (max) and Minimum (min) Values of the Measured and the Optimized Soil Hydraulic Parameters, and the Scaling Factors ($\ln \delta_{\mathrm{PD}}$) for the 84 Soil Samples

	θ_s (cm^3 cm^{-3})	$\ln K_s$ (cm h^{-1})	$\ln h_{m,PD}$ (cm)	σ_{PD}	η_{PD}	$\theta_{r,\mathrm{PD}}$ (cm^3 cm^{-3})	$\ln \delta_{\mathrm{PD}}$
μ	0.53	2.00	5.47	1.90	1.98	0.13	0
STD	0.02	0.72	0.32	0.28	0.39	0.02	0.33
CV (%)	4.73	35.75	5.93	14.83	19.52	16.15	
min	0.46	−0.29	4.70	1.45	0.90	0.03	−1.25
max	0.60	3.50	6.72	3.20	2.87	0.17	0.77

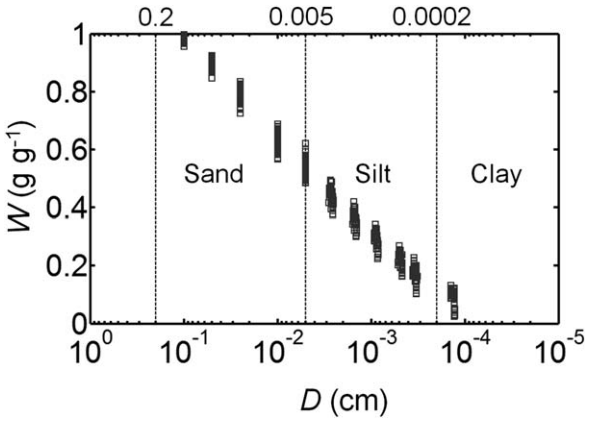

Figure 1. Measured PSDs with five diameter classes determined by the sieving method for sand (0.005 cm $< D <$ 0.2 cm) and six diameter classes determined by the hydrometer method for silt and clay ($D <$ 0.005 cm).

All data were recorded automatically and preprocessed using a data logger.

[23] For each soil sample j, the hydraulic parameters ln $h_{m,\mathrm{PD},j}$, $\sigma_{\mathrm{PD},j}$, $\eta_{\mathrm{PD},j}$, and $\theta_{r,\mathrm{PD},j}$ in equations (2) and (5) (included in the vector $\mathbf{p_{PD}}$) were derived using the MATLAB Optimization Toolbox by minimizing the residuals between observed and fitted soil data included in the following objective function [*Šimůnek and Hopmans*, 2002]:

$$\min_{\mathbf{p_{PD}}} \Phi(\mathbf{p_{PD}}) = \sum_{\omega=1}^{n_{\mathrm{WRF}}} [\theta(h_\omega) - \theta(h_\omega, \mathbf{p_{PD}})]^2 + \xi \sum_{k=1}^{n_{\mathrm{HCF}}} [\log_{10} K_r(h_k) - \log_{10} K_r(h_k, \mathbf{p_{PD}})]^2, \quad (13)$$

where $\theta(h_\omega)$ and $\theta(h_\omega,\mathbf{p_{PD}})$ denote the observed and modeled water retention values, respectively, whereas $\log_{10}[K_r(h_k)]$ and $\log_{10}[K_r(h_k,\mathbf{p_{PD}})]$ are the observed and modeled decimal logarithms of the relative hydraulic conductivity values, respectively, n_{WRF} and n_{HCF} denote the number of observed data pairs for the water retention and relative hydraulic conductivity, respectively. The saturated water content $\theta_{s,j}$ and the saturated hydraulic conductivity $K_{s,j}$ are held fixed at their respective laboratory-measured values. The weighting factor ξ is computed as follows:

$$\xi = \frac{n_{\mathrm{HCF}} \sum_{\omega=1}^{n_{\mathrm{WRF}}} \theta(h_\omega)}{n_{\mathrm{WRF}} \sum_{k=1}^{n_{\mathrm{HCF}}} \log_{10} K_r(h_k)}, \quad (14)$$

ensuring that both data types contribute to the objective function with a virtual equal weight.

4. Results and Discussion

4.1. Simultaneous Scaling From PD

[24] Table 2 presents some basic statistical indices (mean, STD, CV, minimum and maximum values) of the measured (θ_s and ln K_s) and optimized (ln $h_{m,\mathrm{PD}}$, σ_{PD}, η_{PD}, and $\theta_{r,\mathrm{PD}}$) soil hydraulic parameters featuring in equations (2) and (5), together with those derived for the scaling factors ln δ_{PD} calculated from equation (8). For the considered data set, the highest variability occurs, as expected, for the saturated hydraulic conductivity parameter ln K_s, but also for parameter η, with CV of about 36% and 20%, respectively. It is interesting to note that the CV of ln K_s is about twice the value of σ_{PD}, which is an indicator of the pore-size characteristics. Simultaneous scaling results for the directly measured soil hydraulic properties (PD) are presented in Figure 2. Solid black lines in Figures 2c and 2d represent the mean reference soil hydraulic functions (REF-WRF$_{\mathrm{PD}}$ and REF-HCF$_{\mathrm{PD}}$), whereas the open circles indicate both unscaled (Figures 2a and 2b) and scaled WRF$_{\mathrm{PD}}$ (Figure 2c) and HCF$_{\mathrm{PD}}$ (Figure 2d) data pairs, respectively. The scaling theory assumes soil geometric

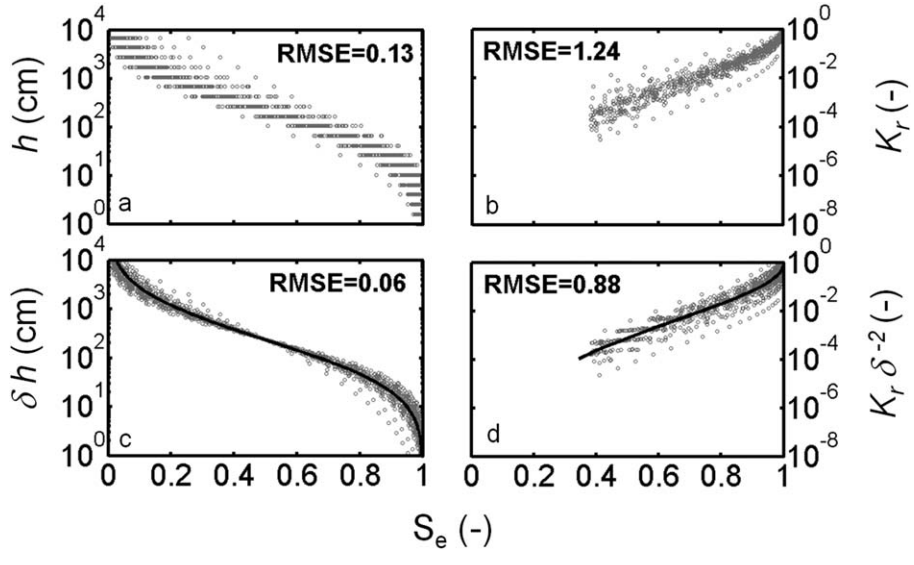

Figure 2. Simultaneous scaling with PD: (a) unscaled WRF$_{\mathrm{PD}}$, (b) unscaled HCF$_{\mathrm{PD}}$, (c) scaled WRF$_{\mathrm{PD}}$, and (d) scaled HCF$_{\mathrm{PD}}$. The black solid lines represent the REF-WRF$_{\mathrm{PD}}$ (Figure 2c) and REF-HCF$_{\mathrm{PD}}$ (Figure 2d), respectively. The RMSE values calculated in equation (15) are also reported.

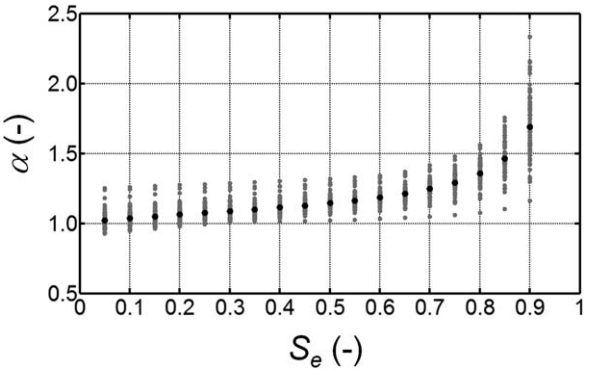

Figure 3. Calibration of the α parameter as a function of the degree of saturation, S_e. The gray dots represent individual calibrations ($\alpha_{i,j}$), whereas black dots represent the average calibration ($\overline{\alpha}_i$) for each $S_{e,i}$ class.

similarity, meaning that soils vary only by their characteristic length (median pore radius) and have identical STDs of the pore size [*Kosugi and Hopmans*., 1998]. This statement ideally presumes that the scaled hydraulic data should perfectly overlie onto their reference functions. Since $\sigma_{\mathrm{PD},j}$ values are not identical (Table 2), the main underlying scaling assumption is violated, hence the scaled hydraulic data cluster around the reference functions. This dispersion is quantified using the root-mean-square error (RMSE) performance diagnostic:

$$\mathrm{RMSE}_{\mathrm{WRF}} = \sqrt{\frac{\sum_{j=1}^{J}\sum_{\omega=1}^{n_{\mathrm{WRF}}}\left[S_e\left(\ln h_{\omega,j}\right) - \hat{S}_e\left(\ln h_{\omega,j}\right)\right]^2}{J \cdot n_{\mathrm{WRF}}}}, \quad (15a)$$

$$\mathrm{RMSE}_{\mathrm{HCF}} = \sqrt{\frac{\sum_{j=1}^{J}\sum_{k=1}^{n_{\mathrm{HCF}}}\left[\log_{10}K_r\left(S_{e,k,j}\right) - \log_{10}\hat{K}_r\left(\hat{S}_{e,k,j}\right)\right]^2}{J \cdot n_{\mathrm{HCF}}}}. \quad (15b)$$

[25] The RMSE values depicted in Figure 2 summarize the effectiveness of the scaling method. The closer the RMSE values to zero, the smaller the distance of the scaled data to the reference curve. The RMSE values of the scaled data are reduced from 0.13 to 0.06 for the WRFs and from 1.24 to 0.88 for the HCFs, respectively. Even though the scaled hydraulic properties are close to the reference functions, significant data scattering remains apparent. However, the CV values of the scaling parameters ln $h_{m,\mathrm{PD}}$ and especially σ_{PD} (see Table 2) can be considered small enough to approximately adhere to the assumption of geometric similar porous media without forcing the user to group the soil samples into different subdata sets [*Das et al*., 2005; *Nasta et al*., 2009].

4.2. Simultaneous Scaling From SD

[26] The soil physical data of PSD and ρ_b are employed, jointly with the direct measurement of θ_s and ln K_s, to predict the scaling results for spatially variable soils. In section 4.2.1, we present the calibration results of the two unknown parameters α and η using the PD of the complete data set. This enables the reference hydraulic functions REF-WRF$_{\mathrm{SD}}$ and REF-HCF$_{\mathrm{SD}}$ to be calculated. Subsequently, in section 4.2.2, the predicted scaling results using the SD will be compared with those computed using the PD (as described in section 4.1). This outcome is certainly the best case scenario and represents the benchmark result from soil texture data. In addition, in section 4.2.3, we evaluate how sensitive the scaling results are with respect to the number of PD employed for the empirical calibration, which is setup to minimize the experimental efforts.

4.2.1. Calibration Procedure

[27] The following steps describe the procedure to calibrate average values of α and η by matching estimated (SD) with measured (PD) reference soil hydraulic functions:

[28] *Step 1: The AP method*. The parameter pairs of Buchan's equation (ln $D_{m,j}$ and $\sigma_{\mathrm{PSD},j}$) retrieved from the 84 samples are used to generate the $D_{i,j}$ values by inverting equation (10) for each jth soil sample using 18 prescribed W_i classes between 0.05 and 0.90 with a step size of 0.05.

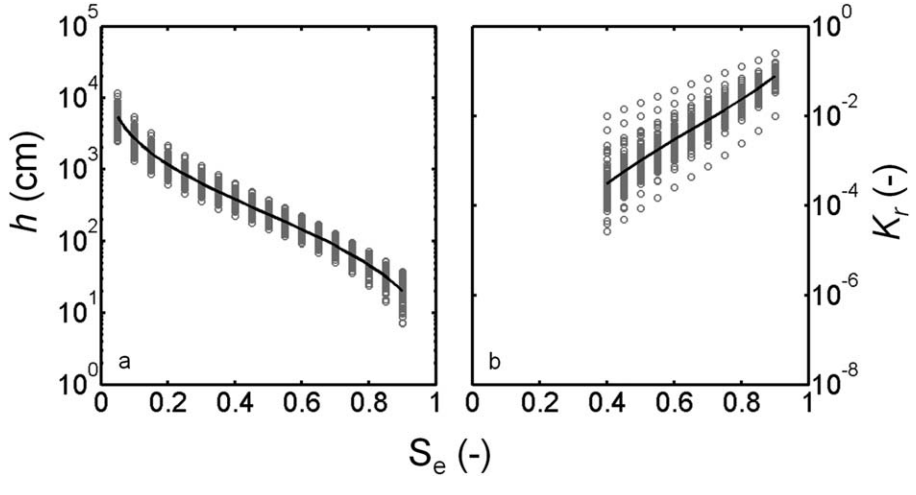

Figure 4. Calibration of the η parameter through the simultaneous optimization of (a) estimated retention data $S_{e,i,j}$-$h_{\mathrm{SD},i,j}$ and (b) measured relative hydraulic conductivity data $S_{e,i,j}$-$K_{r,\mathrm{PD},i,j}$. The black solid lines represent the average hydraulic conductivity functions with the optimized parameters $\overline{h}_m$, $\overline{\sigma}$, and $\overline{\eta}$.

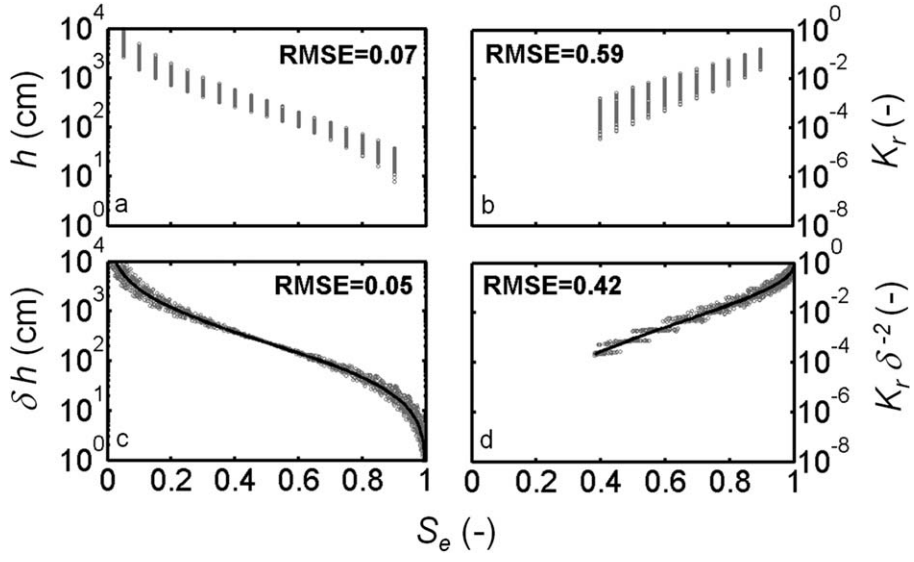

Figure 5. Simultaneous scaling with SD: (a) unscaled WRF_{SD}, (b) unscaled HCF_{SD}, (c) scaled WRF_{SD}, and (d) scaled HCF_{SD}. The black solid lines represent the REF-WRF_{SD} (Figure 5c) and REF-HCF_{SD} (Figure 5d), respectively. The RMSE values calculated in equation (15) are also reported.

We purposely fix the upper limit to 0.90 to avoid instabilities and experimental uncertainties near saturation [*Arya et al*., 1999a]. For each W_i class, $n_{i,j}$ is calculated using equation (11).

[29] *Step 2: Calibration of the parameter* α. Given the assumption of shape similarity between the PSD and the WRF, the empirical calibration involves the direct computation of $\alpha_{i,j}$ for each *j*th soil sample by matching the actual (measured) matric head, $h_{PD,i,j}$ with the corresponding diameter class, $D_{i,j}$ for each prescribed W_i class (or $S_{e,i}$ class). For this purpose, we use the degree of saturation rather than the soil water content to eliminate the effect of the parameter θ_r (CV is about 16%). By inverting equation (12a) and substituting the matric head $h_{PD,i,j}$ with the pore radius $r_{PD,i,j}$ ($r_{PD,i,j} \approx 0.149/h_{PD,i,j}$), we derive [*Vaz et al*., 2005]:

$$\alpha_{i,j} = 1 - \frac{\log_{10}\left[\frac{3}{2e_j}\left(\frac{r_{PD,i,j}}{D_{i,j}/2}\right)^2\right]}{\log_{10}(n_{i,j})}. \quad (16)$$

[30] As previously presented in *Haverkamp et al*. [2002, Fig. 3.3.5-5], we show analogously in Figure 3 the dependency of α on the degree of saturation S_e. The calibration is given by the mean values of $\alpha_{i,j}$ ($\overline{\alpha}_i$) for each prescribed $S_{e,i}$ class (black dots). We point out that $\overline{\alpha}(S_e = 0.5) = 1.14$ (loamy soils) is in agreement with other findings reported in the literature. Specifically, *Arya and Paris* [1981] found an average value of $\alpha = 1.38$ appropriate for coarse soils, whereas later investigations demonstrated average α values of 1.26 for silt loams, 2.10 for sandy clay loams [*Arya et al*., 1982], 0.95 for silt loams, and 1.30 for loams [*Schuh and Cline*, 1990], and α values of 1.46, 1.38, 1.15, 1.16 for sand, sandy loam, loam, silt loam, and clay textures, respectively [*Arya et al*., 1999a]. Note the variation of α with the degree of saturation, $\overline{\alpha}(S_e = 0.05) = 1.02$ and $\overline{\alpha}(S_e = 0.90) = 1.69$. This finding apparently contradicts the trend observed in *Vaz et al*. [2005, Figure 5], yet it is important to consider that α is a calibration parameter that provides an empirical correction for the ideal pore-size distribution represented by a bundle of straight capillary cylindrical tubes.

[31] *Step 3: Calibration of the parameter* η. Using the calibrated $\overline{\alpha}_i$ in equation (12a), the resulting retention data pairs $h_{SD,i,j}$-$S_{e,i}$ can be estimated from the SD (PSD and bulk density). Combining these predicted retention data pairs with their corresponding measured relative conductivity values ($S_{e,i}$-$K_{r,PD,i,j}$), the parameters $\overline{h}_m$, $\overline{\sigma}$, and $\overline{\eta}$ (see Figure 4) are derived using the objective function defined in equation (13). The calibrated value for $\overline{\eta} = 1.94$ is very close to the average value of $\hat{\eta} = 1.98$ presented in Table 2, as obtained from direct measurement of the soil hydraulic properties of all 84 samples.

4.2.2. Predicted Simultaneous Scaling With SD

[32] As the calibration parameters $\overline{\alpha}_i$ and $\overline{\eta}$ are known, we can use the SD to predict the retention and unsaturated HCFs and their spatial variability around the newly estimated reference soil hydraulic functions (REF-WRF_{SD} and REF-HCF_{SD}). The scaling factors of the SD $\delta_{SD,j}$ are computed using equation (8), with the statistical properties of the predicted scaling parameters presented in Table 3.

[33] As expected, mean values of ln $h_{m,SD}$ and σ_{SD} are approximately similar to the original ln $h_{m,PD}$ and σ_{PD} values reported in Table 2; however, the STD values of the predictions of ln $h_{m,SD}$, σ_{SD}, and ln δ_{SD} are reduced with about 50% compared to their corresponding values using primary soil hydraulic data. This result is not surprising. The texture parameters ln D_m and σ_{PSD} (Table 1) exhibit insufficient variability to adequately explain the observed variability of the primary soil hydraulic parameters, which are also affected by soil structure and pore connectivity. We again emphasize that the calibration of α and η purposely adjusts only the estimated mean reference hydraulic properties to guarantee a similar global characterization of the soil domain.

Table 3. Mean (μ), Standard Deviation (STD), Coefficient of Variation (CV), Maximum (max) and Minimum (min) Values of Estimated Soil Hydraulic Parameters and Scaling Factors (ln δ) for the 84 Soil Samples

	ln $h_{m,\mathrm{SD}}$ (cm)	σ_{SD}	ln δ_{SD}
μ	5.47	1.92	0
STD	0.17	0.19	0.17
CV (%)	3.10	9.81	
min	5.12	1.54	−0.37
max	5.84	2.32	0.36

[34] The final predicted scaling results are shown in Figure 5 together with the computed RMSE values for the WRF (equation (15a) and for the HCF (equation (15b)). The RMSE values depicted in Figure 5 (SD) are significantly lower than those previously illustrated in Figure 2 (PD). This outcome is explained by the different basic statistics pertaining to the scaling parameters (ln h_m, σ, and ln δ) observed in Tables 2 (PD) and 3 (SD). The results confirm our previous conclusions that the hybrid scaling method reduces the variation of the predicted WRFs and HCFs. We also note that the effectiveness of the scaling is independent of using either primary or SD, reducing RMSE values from 0.07 to 0.05 after scaling of the WRF and reducing RMSE values from 0.59 to 0.42 after scaling of the HCFs.

[35] We now verify the proposed scaling procedure in Figure 6a by comparing the original unscaled hydraulic conductivity PD $\log_{10}K_{r,\mathrm{PD}}$ with the descaled estimated hydraulic conductivity SD $\log_{10}(\delta^2 K_{r,\mathrm{SD}})$. The best possible outcome would result in alignment of all data along the 1:1 line, if the proposed scaling method was perfect [*Clausnitzer et al.*, 1992]. Our results show reasonable agreement between observations and predictions, with an $R^2 = 0.78$. Scaling errors are quantified by the RDs of individual conductivity pairs:

$$RD = \log_{10}K_{r,\mathrm{PD}} - \log_{10}\left(\delta^2 K_{r,\mathrm{SD}}\right), \tag{17}$$

with their frequency distribution presented in Figure 6b. The bias is relatively small with a mean RD value of −0.022, whereas the standard variation is much less than 1 order of magnitude, with a value of 0.31. The level of success of the proposed scaling is likely partly attributed to the relatively small spatial variability of our data set (Table 1). We would certainly expect less agreement for more heterogeneous databases. Moreover, this hybrid scaling method is designed to maintain the direct measurement of saturated hydraulic conductivity (K_s) to reduce the uncertainty near saturation condition.

4.2.3. Minimum Number of PD Measurements for Calibration

[36] The calibration method described in section 4.2.1 exploits all the direct measurements of the data set and, per definition, should therefore provide the most accurate results. In practice however, a much smaller number of PD might suffice for calibration purposes. In this section, we summarize the results of the calibration procedure for a different number of PD used to adjust the reference soil hydraulic properties.

[37] The number of calibration samples was sequentially increased from 1 to 84 with a step size of 1. For each sample size, 10,000 replicates were randomly generated (without replacement) and the calibration procedure of section 4.2.2 executed. Figure 7a presents the CV values of η (derived from the replicates) as a function of the calibration sample size. As expected, the smaller the number of PD used in the calibration procedure the larger the respective CV values. Logically, if all PD ($J = 84$ samples) are used, the original calibrated mean η value of 1.94 (resulting in section 4.2.2) is derived, with a corresponding CV_η value of zero. For each soil sample size, the calibrated η values were used to calculate the RDs between primary unscaled and estimated descaled hydraulic conductivity data (equation (17)). The results of this analysis are presented in Figure 7b. The values of $\mathrm{CV}_{\mathrm{RD}}$ (derived from the replicates) range between 13% ($j = 1$) and 0% ($J = 84$). It appears that about 15 direct measurements are sufficient for calibration purposes with bias that is less than 5%. Thus, the black reference curves obtained for calibration samples sizes larger than 15 will be sufficiently close to those shown in Figures 5c and 5d, for the entire data set (REF-$\mathrm{WRF}_{\mathrm{SD}}$ and REF-$\mathrm{HCF}_{\mathrm{SD}}$). We conclude that a large part of the uncertainty of

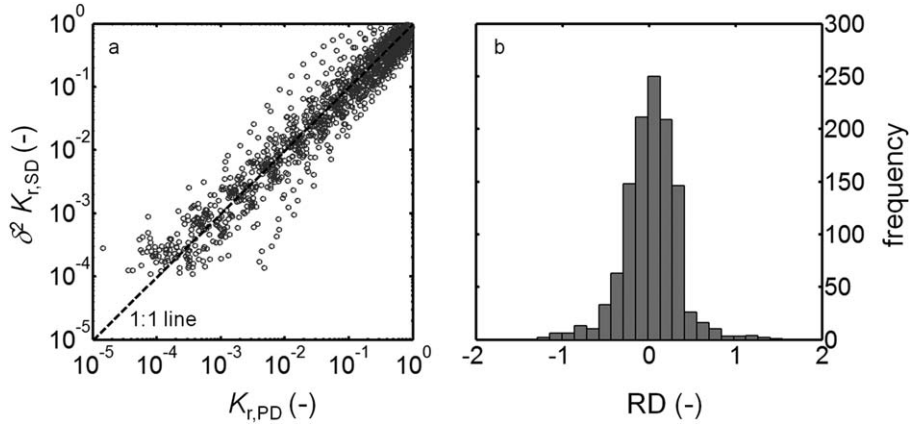

Figure 6. (a) Comparison around the 1:1 line (dashed line) between original unscaled relative hydraulic conductivity data $K_{r,\mathrm{PD}}$ and estimated descaled relative hydraulic conductivity data $\delta^2 K_{r,\mathrm{SD}}$ and (b) frequency distribution of the RD values.

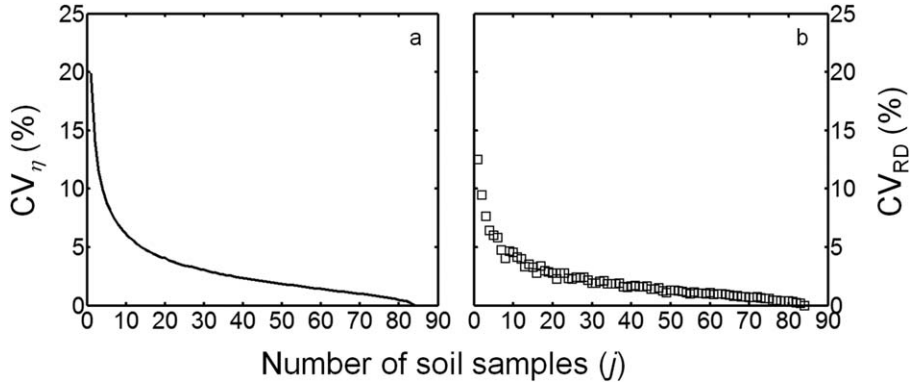

Figure 7. (a) CV of calibrated η (CV_η) as a function of the number of soil samples and (b) CV of corresponding RD (CV_{RD}) as a function of the number of soil samples.

the proposed hybrid scaling method is determined by the reduced variability in scaling factors estimated from PSD measurements as compared with those computed directly from laboratory measurement of the PD.

[38] The results presented in Figure 7 help to judge how many samples are needed for calibration purposes. Yet, the results pertain directly to the data set being used herein. It should be evident that if the spatial variability increases, so does the required number of calibration samples [*Nasta et al*., 2009].

5. Conclusions

[39] The scaling approach of *Miller and Miller* [1956] is still widely employed to characterize the spatial variability of soil hydraulic properties. This technique seems particularly appealing as it provides the opportunity to stochastically generate new soil hydraulic parameters in unknown locations of a study area through the lognormal pdf of the scaling factors and the corresponding reference soil hydraulic properties [*Nasta et al.*, 2013]. Successful applications of this procedure to real cases require a relatively large number of soil samples for large-scale hydrological applications. This task is rather expensive, time consuming, and labor intensive. To characterize the spatial variation of soil hydraulic properties, in this paper, we have developed an alternative hybrid scaling approach that uses more easily to be determined secondary soil data coupled with easily obtainable PD (such as saturated soil water content and saturated hydraulic conductivity).

[40] This study is a followup of the work presented by *Nasta et al*. [2009], providing the prediction of both water retention and unsaturated HCFs. The proposed method is a compromise between effectiveness in describing the soil spatial variation over relatively larger scales and the sustainability of experimental efforts. However, we caution on the potential issues affecting this method since soil texture measurements are generally insufficient to explain all observed spatial variations in soil hydraulic functions, especially the hydraulic conductivity characteristic.

[41] A possible way to overcome this limitation in our hybrid scaling method is to consider bimodal hydraulic relationships in lieu of the conventional unimodal forms of Kosugi's WRF and HCF. Such functions would better describe the effect of soil structure near saturation [*Romano et al*., 2011].

Notation

CV	coefficient of variation.
D	particle diameter (L).
e	soil void ratio ($L^3\ L^{-3}$).
$G(S_e)$	connectivity factor.
h	soil matric potential head (L).
HCF	hydraulic conductivity function.
i	counter for soil particle diameter class.
j	counter for soil sample.
k	counter for hydraulic conductivity data pairs.
K	soil hydraulic conductivity ($L\ T^{-1}$).
K_r	relative hydraulic conductivity.
K_s	saturated hydraulic conductivity ($L\ T^{-1}$).
l	tortuosity-connectivity factor.
$\ln D_m$	log-transformed particle diameter (L).
$\ln h_m$	mean log-transformed matric potential head (L).
$\ln r_m$	mean log-transformed pore radius (L).
max	maximum value.
min	minimum value.
n	number of solid particles (M^{-1}).
n_{HCF}	number of observed hydraulic conductivity data pairs.
n_{WRF}	number of observed water retention data pairs.
PD	primary data.
pdf(r)	probability density function of soil pore radii (L^{-1}).
PSD	particle-size distribution.
r	pore radius (L).
RMSE	root-mean-square error.
SD	secondary data.
S_e	degree of saturation.
STD	standard deviation.
$T(S_e)$	tortuosity factor.
W	solid mass fraction ($M\ M^{-1}$).
WRF	water retention function.
α	empirical parameter.
δ	scaling factor.
ε	soil porosity ($L^3\ L^{-3}$).
η	conductivity parameter.
μ	mean value.

θ soil water content ($L^3\,L^{-3}$).
θ_r residual water content ($L^3\,L^{-3}$).
θ_s saturated water content ($L^3\,L^{-3}$).
ρ_b oven-dry bulk density ($M\,L^{-3}$).
ρ_s soil particle density ($M\,L^{-3}$).
σ standard deviation of log-transformed matric potential head.
σ_{PSD} standard deviation of log-transformed particle diameter.
ω counter for water retention data pairs.
ξ weighting factor.

[42] **Acknowledgments.** The first author wishes to thank Vanessa Carfora and Antonella Puglia for their precious technical support. The comments and suggestions of the three anonymous reviewers are greatly appreciated and have significantly enhanced the current version of this manuscript.

References

Arya, L. M., and J. L. Heitman (2010), Hydraulic conductivity function from water flow similarity in idealized- and natural-structure pores, *Soil Sci. Soc. Am. J.*, *74*, 787–796.

Arya, L. M., and J. F. Paris (1981), A physico-empirical model to predict the soil moisture characteristic from particle-size distribution and bulk density data, *Soil Sci. Soc. Am. J.*, *45*, 1023–1030.

Arya, L. M., J. C. Ritchter, and S. A. Davidson (1982), A comparison of soil moisture characteristic predicted by the Arya-Paris model with laboratory-measured data, AgRISTARS Tech. Rep. SM-L1–04247, JSC-17820, NASA-Johnson Space Cent., Houston, Tex.

Arya, L. M., F. J. Leij, M. Th. van Genuchten, and P. Shouse (1999a), Scaling parameter to predict the soil water characteristic from particle-size distribution data, *Soil Sci. Soc. Am. J.*, *63*, 510–519.

Arya, L. M., F. J. Leij, P. Shouse, and M. Th. van Genuchten (1999b), Relationship between hydraulic conductivity function and particle-size distribution, *Soil Sci. Soc. Am. J.*, *63*, 1063–1070.

Arya, L. M., D. C. Bowman, B. B. Thapa, and D. K. Kassel (2008), Scaling soil water characteristics of golf course and athletic field sands from particle-size distribution, *Soil Sci. Soc. Am. J.*, *72*, 25–32.

Assouline, S. (2001), A model for soil relative hydraulic conductivity based on the water retention characteristic curve, *Water Resour. Res.*, *37*, 265–271.

Assouline, S. (2005), On the relationship between the pore size distribution index and characteristics of the soil hydraulic functions, *Water Resour. Res.*, *41*, W07019, doi:10.1029/2004WR003511.

Bah, A. R., O. Kravchuk, and G. Kirchhof (2009), Fitting performance of particle-size distribution models on data derived by conventional and laser diffraction techniques, *Soil Sci. Soc. Am. J.*, *73*, 1101–1107.

Basile, A., and G. D'Urso (1997), Experimental corrections of simplified methods for predicting water retention curves in clay-loamy soils from particle-size determination, *Soil Technol.*, *10*, 261–272.

Blank, L. A., A. G. Hunt, and T. E. Skinner (2007), A numerical procedure to calculate hydraulic conductivity for an arbitrary pore size distribution, *Vadose Zone J.*, *7*, 461–472.

Brutsaert, W. (2000), A concise parameterization of the hydraulic conductivity of unsaturated soils, *Adv. Water Resour.*, *23*, 811–815.

Buchan, G. D. (1989), Applicability of the simple lognormal model to particle-size distribution in soils, *Soil Sci.*, *147*, 155–161.

Buczko, U., and H. H. Gerke (2005), Evaluation of the Arya-Paris model for estimating water retention characteristics of lignitic mine soils, *Soil Sci.*, *170*, 483–494.

Chan, T. P., and R. S. Govindaraju (2004), Estimating soil water retention curve from particle-size distribution data based on polydisperse sphere systems, *Vadose Zone J.*, *3*, 1443–1454.

Chaudhari, S. K., and R. K. Batta (2003), Predicting unsaturated hydraulic conductivity functions of three Indian soils from particle size distribution data, *Aust. J. Soil Res.*, *41*, 1457–1466.

Chirico, G. B., H. Medina, and N. Romano (2007), Uncertainty in predicting soil hydraulic properties at the hillslope scale with indirect methods, *J. Hydrol.*, *334*, 405–422.

Ciollaro, G., and N. Romano (1995), Spatial variability of the hydraulic properties of a volcanic soil, *Geoderma*, *65*, 263–282.

Clausnitzer, V., J. W. Hopmans, and D. R. Nielsen (1992), Simultaneous scaling of soil water retention and hydraulic conductivity curves, *Water Resour. Res.*, *28*, 19–31.

Coleman, T. F., and Y. Li (1996), An interior, trust region approach for nonlinear minimization subject to bounds, *SIAM J. Optim.*, *6*, 418–445.

Das, B.S., N. W. Haws, and P. S. C. Rao (2005), Defining geometric similarity in soils, *Vadose Zone J.*, *4*, 264–270.

Gee, G.W., and D. Or (2002), Particle-size analysis, in *Methods of Soil Analysis, Part 4: Physical Methods, SSSA Book Ser.*, vol. *5*, edited by J. H. Dane, and G. C. Topp, pp. 255–293, Madison, Wis.

Hayashi, Y., K. Kosugi, and T. Mizuyama (2009), Soil water retention curves characterization of a natural forested hillslope using a scaling technique based on a log-normal pore-size distribution, *Soil Sci. Soc. Am. J.*, *73*, 55–64.

Haverkamp, R., P. Reggiani, and J. R. Nimmo (2002), Property-transfer models, in *Methods of Soil Analysis, Part 4, SSSA Book Ser.*, vol. *5*, edited by J. H. Dane, and G. C. Topp, pp. 759–782, SSSA, Madison, Wis.

Hendrayanto, K. Kosugi, and T. Mizuyama (2000), Scaling hydraulic properties of forest soils, *Hydrol. Processes*, *14*, 521–538.

Hopmans, J. W., D. R. Nielsen, and K. L. Bristow (2002a), How useful are small-scale soil hydraulic property measurements for large-scale vadose zone modeling, in *Heat and Mass Transfer in the Natural Environment, The Philip Volume, Geophys. Monogr. Ser.*, vol. *129*, edited by D. Smiles, P. A. C. Raats, and A. Warrick, pp. 247–258, AGU, Washington, D. C.

Hopmans, J. W., J. Šimůnek, N. Romano, and W. Durner (2002b), Inverse methods, in *Methods of Soil Analysis, Part 4, SSSA Book Ser.*, vol. *5*, edited by J. H. Dane and G. C. Topp, pp. 963–1008, SSSA, Madison, Wis.

Hwang, S. I., and S. I. Choi (2006), Use of a lognormal distribution model for estimating soil water retention curves from particle-size distribution data, *J. Hydrol.*, *323*, 325–334.

Hwang, S. I., and S. P. Hong (2006), Estimating relative hydraulic conductivity from lognormally distributed particle-size data, *Geoderma*, *133*, 421–430.

Kosugi, K. (1996), Log-normal distribution model for unsaturated soil hydraulic properties, *Water Resour. Res.*, *32*, 2697–2703.

Kosugi, K., and J. W. Hopmans (1998), Scaling water retention curves for soils with lognormal pore-size distribution, *Soil Sci. Soc. Am. J.*, *62*, 1496–1505.

Kosugi, K., J. W. Hopmans, J. H. Dane (2002), Parametric models, in *Methods of Soil Analysis, Part 4, SSSA Book Ser.* vol. *5*, edited by J. H. Dane and G. C. Topp, pp. 739–757, SSSA, Madison, Wis.

Lebeau, M., and J.-M. Konrad (2010), A new capillary and thin film flow for predicting the hydraulic conductivity of unsaturated porous media, *Water Resour. Res.*, *46*, W12554, doi:10.1029/2010WR009092.

Leij, F. J., W. B. Russell, and S. M. Lesch (1997), Closed form expressions for water retention and conductivity data, *Ground Water*, *35*(5), 848–858.

Miller, E. E., and R. D. Miller (1956), Physical theory of capillary flow phenomena, *J. Appl. Phys.*, *27*, 324–332.

Minasny, B., and A. B. McBratney (2007), Spatial prediction of soil properties using EBLUP with the Matérn covariance function, *Geoderma*, *140*, 324–336.

Mohanty, B. P., and J. Zhu (2007), Effective hydraulic parameters in horizontally and vertically heterogeneous soils for steady-state land-atmosphere interaction, *Am. Meteorol. Soc.*, *8*, 715–729, doi:10.1175/JHM606.1.

Mualem, Y. (1976), A new model for predicting the hydraulic conductivity of unsaturated porous media, *Water Resour. Res.*, *12*, 513–522.

Nasta, P., T. Kamai, G. B. Chirico, J. W. Hopmans, and N. Romano (2009), Scaling soil water retention functions using particle-size distribution, *J. Hydrol.*, *374*, 223–234.

Nasta, P., N. Romano, and G. B. Chirico (2013), Functional evaluation of a simplified scaling method for assessing the spatial variability of soil hydraulic properties at the hillslope scale, *Hydrol. Sci. J.*, *58*, 1–13.

Nimmo, J. R., W. N. Herkelrath, and A. M. Laguna Luna (2007), Physically based estimation of soil water retention from textural data: general framework, new models, and streamlined existing models, *Vadose Zone J.*, *6*, 766–773.

Pachepsky, Y. A., and W. J. Rawls (2004), Status of pedotransfer functions, in *Development of Pedotransfer Functions in Soil Hydrology*, Dev. in Soil Sci., vol. *30*, edited by Y. A. Pachepsky and W. J. Rawls, pp. vii-xvi, Elsevier Sci. B.V., Amsterdam, The Netherlands.

Peters, A., and W. Durner (2008), Simplified evaporation method for determining soil hydraulic properties, *J. Hydrol.*, *356*, 147–162.

Peters, A., W. Durner, and G. Wessolek (2011), Consistent parameter constraints for soil hydraulic functions, *Adv. Water Resour.*, *34*, 1352–1365.

Reynolds, W. D., and D. E. Elrick (2002), Saturated and field-saturated water flow parameters: Falling head soil core (tank) method, in *Methods of Soil Analysis, Part 4: Physical Methods, SSSA Book Ser.* vol. *5*, edited by J. H. Dane and G. C. Topp, pp. 809–812, SSSA, Madison, Wis.

Romano, N. (1993), Use of an inverse method and geostatistics to estimate soil hydraulic conductivity for spatial variability analysis, *Geoderma*, *60*, 169–186.

Romano, N. (2004), Spatial structure of PTF estimates, in *Development of Pedotransfer Functions in Soil Hydrology*, edited by Y. A. Pachepsky and W. J. Rawls, pp. 295–319, Elsevier Sci. B.V.

Romano, N., and A. Santini (1999), Determining soil hydraulic functions from evaporation experiments by a parameter estimation approach: Experimental verifications and numerical studies, *Water Resour. Res.*, *35*, 3343–3359.

Romano, N., P. Nasta, G. Severino, and J. W. Hopmans (2011), Using bimodal log-normal functions to describe soil hydraulic properties, *Soil Sci. Soc. Am. J.*, *75*, 468–480.

Schaap, M. G., and W. Bouten (1996), Modeling water retention curves of sandy soils using neural networks, *Water Resour. Res.*, *32*, 3033–3040.

Schaap, M. G., F. J. Leij, and M. Th. van Genuchten (1998), Neural network analysis for hierarchical prediction of soil water retention and saturated hydraulic conductivity, *Soil Sci. Soc. Am. J.*, *62*, 847–855.

Šimůnek, J., and J.W. Hopmans (2002), Parameter optimization and nonlinear fitting, in *Methods of Soil Analysis, Part 4, SSSA Book Ser.*, vol. *5*, J. H. Dane and G. C. Topp, pp. 139–157, SSSA, Madison, Wis.

Schuh, W. M., and R. L. Cline (1990), Effect of soil properties on unsaturated hydraulic conductivity pore-interaction factors, *Soil Sci. Soc. Am. J.*, *50*, 848–855.

Tietje, O., and M. Tapkenhinrichs (1993), Evaluation of pedo-transfer functions, *Soil Sci. Soc. Am. J.*, *57*, 1088–1095.

Tillotson, P. M., and D. R. Nielsen (1984), Scale factors in soil science, *Soil Sci. Soc. Am. J.*, *48*, 953–959.

Topp, C. G., and P. A. Ferré (2002), Methods for measurement of soil water content: thermogravimetric using convective oven-drying, in *Methods of Soil Analysis, Part 4: Physical Methods, SSSA Book Ser.*, vol. *5*, edited by J. H. Dane and G. C. Topp, pp. 422–424, SSSA, Madison, Wis.

Touma, J. (2009), Comparison of the soil hydraulic conductivity predicted from its water retention expressed by the equation of van Genuchten and different capillary models, *Eur. J. Soil Sci.*, *60*, 671–680.

Tuli, A., K. Kosugi, and J. W. Hopmans (2001), Simultaneous scaling of soil water retention and unsaturated hydraulic conductivity functions assuming lognormal pore-size distribution, *Adv. Water Resour.*, *24*, 677–688.

Vaz, C. M. P., M. d. F. Iossi, J. d. M. Naime, A. Macero, J. M. Reichert, D. J. Reinert, and M. Cooper (2005), Validation of the Arya and Paris water retention model for Brazilian soils, *Soil Sci. Soc. Am. J.*, *69*, 577–583.

Vereecken, H., R. Kasteel, J. Vanderborght, T. and Harter (2007), Upscaling hydraulic properties and soil water flow processes in heterogeneous soils: A review, *Vadose Zone J.*, *6*, 1–28.

Vereecken, H., M. Weynants, M. Javaux, Y. Pachepsky, M. G. Schaap, and M. Th. van Genuchten (2011), Using pedotransfer functions to estimate the van Genuchten-Mualem soil hydraulic properties: A review, *Vadoze Zone J.*, *9*, 795–820.

Vrugt, J. A., G. Schoups, J. W. Hopmans, C. Young, W. W. Wallender, T. Harter, and W. Bouten (2004), Inverse modeling of large-scale spatially distributed vadose zone properties using global optimization, *Water Resour. Res.*, *40*, W06503, doi:10.1029/2003WR002706.

Zhu, J., and B. P. Mohanty (2002), Upscaling of soil hydraulic properties for steady state evaporation and infiltration, *Water Resour. Res.*, *38*(9), 1178, doi:10.1029/2001WR000704.

Zhu, J., and B. P. Mohanty (2003), Effective hydraulic parameters for steady state vertical flow in heterogeneous soils, *Water Resour. Res.*, *39*(8), 1227, doi:10.1029/2002WR001831.

Warrick, A. W., and D. R. Nielsen (1980), Spatial variability of soil physical properties in the field, in *Applications of Soil Physics*, edited by D. Hillel, pp. 319–344, Academic Press, New York.

Wendroth, O., W. Ehlers, J. W. Hopmans, H. Kage, J. Halbertsma, and J. H. M. Wösten, (1993), Re-evaluation of the evaporation method for determining hydraulic functions in unsaturated soils, *Soil Sci. Soc. Am. J.*, *57*, 1436–1443.

Weynants, M., H. Vereecken, and M. Javaux (2009), Revisiting Vereecken pedotransfer functions: Introducing a closed-form hydraulic model, *Vadose Zone J.*, *8*, 86–95.